Protein Folding Thermodynamics Applied to the Photocycle of the Photoactive Yellow Protein

Marion E. Van Brederode,* Wouter D. Hoff,* Ivo H. M. Van Stokkum,# Marie-Louise Groot,# and Klaas J. Hellingwerf*

*Department of Microbiology, E. C. Slater Institute, BioCentrum, University of Amsterdam, 1018 WS Amsterdam, and #Department of Physics and Astronomy, Free University, 1081 HV Amsterdam, The Netherlands

ABSTRACT Two complementary aspects of the thermodynamics of the photoactive yellow protein (PYP), a new type of photoreceptor that has been isolated from *Ectothiorhodospira halophila*, have been investigated. First, the thermal denaturation of PYP at pH 3.4 has been examined by global analysis of the temperature-induced changes in the UV-VIS absorbance spectrum of this chromophoric protein. Subsequently, a thermodynamic model for protein (un)folding processes, incorporating heat capacity changes, has been applied to these data. The second aspect of PYP that has been studied is the temperature dependence of its photocycle kinetics, which have been reported to display an unexplained deviation from normal Arrhenius behavior. We have extended these measurements in two solvents with different hydrophobicities and have analyzed the number of rate constants needed to describe these data. Here we show that the resulting temperature dependence of the rate constants can be quantitatively explained by the application of a thermodynamic model which assumes that heat capacity changes are associated with the two transitions in the photocycle of PYP. This result is the first example of an enzyme catalytic cycle being described by a thermodynamic model including heat capacity changes. It is proposed that a strong link exists between the processes occurring during the photocycle of PYP and protein (un)folding processes. This permits a thermodynamic analysis of the light-induced, physiologically relevant, conformational changes occurring in this photoreceptor protein.

INTRODUCTION

A photoactive yellow protein (PYP) has been isolated from *Ectothiorhodospira halophila*, *Rhodospirillum salexigens*, and *Chromatium salexigens* (Meyer, 1985; Meyer et al., 1990; Meyer et al., unpublished results; Hoff et al., 1994b). Evidence has been obtained from *Ectothiorhodospira halophila* that PYP functions as the photoreceptor for the negative phototactic response of this organism toward blue light (Sprenger et al., 1993). PYP is a 14-kDa water-soluble protein that is very stable toward denaturation. The visible absorption spectrum of PYP consists of a strong, slightly asymmetric broad band, peaking at 446 nm (Meyer, 1985). At pH values below 3, PYP is reversibly converted from the ground state to a bleached state, absorbing maximally at approximately 345 nm (Meyer et al., 1987). At neutral pH, after absorption of a blue photon, the protein-chromophore complex undergoes a number of dark transformations, in which PYP changes its absorption spectrum and eventually returns to the initial ground state. This photocycle and other photophysical/chemical characteristics of PYP strongly resemble those observed in the (archaebacterial) rhodopsins (Meyer et al., 1987, 1991; Stavenga et al., 1991; Hoff et al., 1992, 1994c). However, the chromophoric group of PYP is different from the retinal chromophore present in rhodopsins and is not attached to the apoprotein via a Schiff base linkage to a lysine residue, but rather is linked to a cysteine residue (Van Beeumen et al., 1993). The chemical structure of the chromophore of PYP has recently been elucidated to be *p*-coumaric acid, establishing PYP as a new type of photoreceptor (Hoff et al., 1994a; Baca et al., 1994). Furthermore, the three-dimensional structure of PYP is completely different from that of the bacterial rhodopsins. The crystal structure of PYP has recently been determined at 1.4 Å resolution, showing that it consists of an α/β-fold that is reminiscent of a number of eukaryotic proteins involved in signal transduction (Borgstahl et al., 1995). This revises the original 2.4 Å crystal structure (McRee et al., 1989). In contrast, rhodopsins are all-helical transmembrane proteins (Henderson et al., 1990). The amino acid sequence of PYP (125 amino acids) shows no obvious sequence similarity to any other protein available in the databases (Van Beeumen et al., 1993).

In the photocycle of PYP, in the time domain between 2 ns and 2 s, two intermediates have been identified. After a short light flash, a red-shifted intermediate is formed within 1 ns, which is converted into a blue-shifted intermediate that returns to the ground state within 1 s (Meyer et al., 1987, 1989, 1991; Hoff et al., 1994c). Here we call the red-shifted intermediate pR and the blue-shifted intermediate pB. The ground state will be designated pG and the blue-shifted state resulting from acid or temperature denaturation pB_{dark}. Fig. 8 *A* shows a scheme of the PYP photocycle.

Received for publication 30 October 1995 and in final form 3 April 1996.

Address reprint requests to Dr. Klaas J. Hellingwerf, Department of Microbiology, University of Amsterdam, E. C. Slater Institute, BioCentrum Amsterdam, Nieuwe Achtergracht 127, 1018 WS Amsterdam, The Netherlands. Tel.: 020-525-7054; Fax: 31-20-525-7056; E-mail: a471hell@horus.sara.nl.

Ms. Van Brederode's present address is Department of Biophysics, Faculty of Physics and Astronomy, Free University, De Boelelaan 1081, 1081 HV Amsterdam, The Netherlands.

0006-3495/96/07/365/16 $2.00

The effect of solvent hydrophobicity and viscosity on the photocycle kinetics of PYP has been determined (Meyer et al., 1989). From the effect of viscosity on the photocycle kinetics it has been concluded that PYP undergoes a conformational change during progression through its photocycle. The effect of solvent hydrophobicity on the photocycle kinetics indicates that pB exposes more hydrophobic surface area to the solvent than pR and pG, because increased hydrophobicity of the solvent (achieved by the addition of various aliphatic monofunctional alcohols, ranging from methanol to *n*-butanol) accelerates the pR-to-pB transition and decreases the rate constant of pB back to pG (Meyer et al., 1989). Salamon et al. (1995) showed that this increased hydrophobicity promotes binding of PYP to lipid bilayers.

The temperature dependence of the photocycle kinetics of PYP has been determined, assuming monoexponential transitions (Meyer et al., 1989). The last step of the photocycle, the recovery of pG from pB, shows a highly unusual temperature dependence: the reaction speeds up twofold between 5 and 35°C and then slows down threefold upon a further temperature increase to 62°C. Therefore, at temperatures above 35°C the apparent activation energy, resulting from the Arrhenius plot of this transition, is negative. It was proposed that the change in slope reflects a temperature-induced transition of pB, which would result in an altered kinetic behavior (Meyer et al., 1989). However, it is not obvious how this phenomenon would lead not only to a change in the magnitude of the activation energy, but also to a change of its sign. In contrast to the transition from pB to pG, the transition from pR to pB has been reported to show normal Arrhenius behavior (Meyer et al., 1989).

Here we report detailed kinetic measurements of the PYP photocycle over the temperature range from 5 to 60°C, with and without the addition of 3% (v/v) butanol. It is shown that the unusual temperature dependence of the pB-to-pG transition can be quantitatively described with a thermodynamic model in which the effect of a heat capacity change during the transition is considered. Such a model was developed to describe the equilibrium thermodynamics of protein folding and unfolding (see Brandts, 1964; Privalov, 1979, 1988, 1992; Chen and Schellman, 1989). An extension of this model yields a description of the kinetics of a protein folding process by taking into account heat capacity changes in transition state theory (see Chen et al., 1989).

THEORETICAL MODEL

Thermodynamic analysis of the reversible thermal denaturation of PYP

In a folded water-soluble protein most of the hydrophobic amino acids are buried within the hydrophobic core of the protein, and most of the hydrophilic amino acid side chains are exposed to the solvent. In the unfolded random coil conformation, all residues become exposed to the solvent. To describe protein conformational changes thermodynamically, it is necessary to take into account the fact that unfolding of a water-soluble protein is accompanied by an increment in the heat capacity of the solution. The exposure of hydrophobic amino acid side chains upon protein unfolding is the main contributor to this heat capacity increase; its value is different for different proteins and correlates well with the surface area of exposed nonpolar groups upon unfolding of the protein (Makhatadze and Privalov, 1990; Privalov and Makhatadze, 1990). The difference in heat capacity between a folded and an unfolded protein can be determined by scanning microcalorimetry (Privalov and Potekhin, 1986). A direct consequence of the heat capacity increase (ΔC_p) upon protein unfolding is that the thermodynamic parameters that describe the transition are temperature dependent, because

$$\frac{\partial \Delta H}{\partial T} = \Delta C_p \tag{1}$$

$$\frac{\partial \Delta S}{\partial T} = \frac{\Delta C_p}{T}, \tag{2}$$

where ΔH and ΔS are the enthalpy and entropy difference between the two states considered, and T is the absolute temperature. Assuming that the heat capacity difference ΔC_p between the two states does not change with temperature (see Discussion), integration of Eqs. 1 and 2 leads to the following equations:

$$\Delta H(T) = \Delta H(T_0) - (T_0 - T)\Delta C_p \tag{3}$$

$$\Delta S(T) = \Delta S(T_0) - \Delta C_p \ln\left(\frac{T_0}{T}\right), \tag{4}$$

in which T_0 can be any reference temperature.

Summing Eqs. 3 and 4 in the equation for the free energy,

$$\Delta G = \Delta H - T\Delta S, \tag{5}$$

leads to

$$\Delta G(T) = \Delta H(T_0) - (T_0 - T)\Delta C_p - T\left(\Delta S(T_0) + \Delta C_p \ln\left(\frac{T}{T_0}\right)\right). \tag{6}$$

The temperature dependence of the natural logarithm of the equilibrium constant K for the reaction between the native and the denatured states of the protein then equals

$$\ln K = \frac{\Delta S(T_0)}{R} - \frac{\Delta H(T_0)}{RT} - \frac{\Delta C_p}{R}\left(1 - \frac{T_0}{T} + \ln\frac{T_0}{T}\right). \tag{7}$$

Equation 7 has been used to analyze the thermal denaturation of PYP by means of linear regression, in which for a fixed value of T_0 the parameters $\Delta S(T_0)$, $\Delta H(T_0)$, and ΔC_p were estimated.

A thermodynamic model of the PYP photocycle: transition state theory and heat capacity changes

Based on the effect of hydrophobicity on the photocycle kinetics of PYP, Meyer et al. have proposed that pB exposes more hydrophobic surface area than pR or pG (see above, Meyer et al., 1989). A more precise conclusion is that pB exposes more hydrophobic surface area to the solvent than the activated state $pB^{\#}$ (see Fig. 8) and that pR exposes less hydrophobic surface area to the solvent than the activated $pR^{\#}$, because according to transition state theory (see Laidler, 1987), a reaction rate is only determined by the activation equilibrium constant between the ground state(s) and the transition state(s) of the reactant(s). Because the exposure of hydrophobic surface area to water induces a heat capacity increase, we propose that the transition-state $pR^{\#}$ has a higher heat capacity than pR and that the activated-state $pB^{\#}$ has a lower heat capacity than pB. The description of the photocycle kinetics in thermodynamic terms therefore requires the combination of two theoretical considerations. First, through transition state theory a link is made between thermodynamics and kinetics. And second, the thermodynamic effects of heat capacity changes have to be incorporated, as was done for the equilibrium processes (see above).

Transition state theory (see Laidler, 1987) assumes that an equilibrium exists between the reactant(s) and the transition state of the reactant(s), which determines the reaction rate. For the photocycle of PYP this means that an equilibrium exists between pB and the transition state, $pB^{\#}$, and between pR and the transition state, $pR^{\#}$:

$$\frac{[pR^{\#}]}{[pR]} = K_1^{\#} \tag{8}$$

$$\frac{[pB^{\#}]}{[pB]} = K_2^{\#}, \tag{9}$$

where $K_i^{\#}$ is the activation equilibrium constant of the ith reaction (subscripts 1 and 2 indicate the pR-to-pB transition and the pB-to-pG transition, respectively). These activation equilibrium constants are characterized by an activation free energy difference

$$\Delta G_i^{\#} = -RT \ln K_i^{\#}. \tag{10}$$

The rate constant k_i and the activation free energy change, $\Delta G_i^{\#}$, are related by the Eyring equation

$$k_i = \kappa \nu \exp\left(\frac{-\Delta G_i^{\#}}{RT}\right), \tag{11}$$

in which κ is the transmission coefficient that determines the transition probability with which the activated state is converted to the product and ν is a vibrational frequency, which is given by $k_B T/\hbar$ for a monomolecular reaction (see Devault, 1980), with k_B and $\hbar$ being the Boltzmann and Planck constants, respectively. When the transmission coefficient equals 1, as it does for adiabatic reactions, the equilibrium activation constant is given by

$$K_i^{\#} = \frac{k_i \hbar}{k_b T}. \tag{12}$$

The expression for the activation equilibrium constant, which will be used below to analyze the temperature dependence of the PYP photocycle kinetics, is given by

$$\ln K_i^{\#} = \frac{\Delta S_i^{\#}(T_0)}{R} - \frac{\Delta H_i^{\#}(T_0)}{RT} - \frac{\Delta C_{pi}^{\#}}{R}\left(1 - \frac{T_0}{T} + \ln \frac{T_0}{T}\right) \tag{13}$$

(compare with the derivation leading to Eq. 7), in which $\Delta S_i^{\#}$, $\Delta H_i^{\#}$, and $\Delta G_i^{\#}$ are the entropy, enthalpy, and heat capacity changes of activation.

These thermodynamic parameters can be obtained from a fit of the temperature dependence of the reaction rates k_i. Equation 13 predicts that a function of $1/T$ is linear when $\Delta C_p^{\#}$ is zero and has a positive curvature when $\Delta C_p^{\#}$ is negative and a negative curvature when $\Delta C_p^{\#}$ is positive. Thus, with the model proposed here, the reported non-Arrhenius behavior of the transition from pB to pG is actually predicted. It is remarkable that the transition from pR to pB was reported to show linear Arrhenius behavior, especially because the effect of hydrophobicity on the photocycle kinetics of the pR-to-pB transition is of the same order of magnitude, but of opposite sign, as of the pB-to-pG transition (Meyer et al., 1989). However, it depends on the value of $\Delta C_p^{\#}$, in combination with those of $\Delta S_i^{\#}$, $\Delta H_i^{\#}$, and $\Delta G_i^{\#}$, whether or not a maximum or a minimum is actually observed in the experimentally accessible temperature range. Here we report the temperature dependence of both transitions in PYP in 10 mM Tris-HCl (pH 7.5) and in the more hydrophobic solvent 10 mM Tris-HCl (pH 7.5) plus 3% (v/v) butanol, and analyze it with Eq. 13. In addition, equilibrium studies of the transitions in PYP are reported. The results of these analyses are compared with the results of thermodynamic investigations of protein folding and unfolding processes.

MATERIALS AND METHODS

Sample preparation

PYP was isolated from *E. halophila* cells, essentially as described by Meyer (1985), with the following modifications. The cells were broken by sonification, and size exclusion chromatography was performed by fast protein liquid chromatography. The quality of the sample, after isolation and during the experiments, was assessed by measuring UV-VIS spectra on an Aminco DW-2000 spectrophotometer (SLM Instruments) or a Cary 219 spectrophotometer (Varian) and by electrospray ionization mass spectrometry (see Van Beeumen et al., 1993). The PYP samples used in this study were purified to homogeneity and were fully intact according to the analyses with these methods.

Equilibrium measurements

Purified PYP was dissolved in 25 mM citrate, 10 mM Tris-HCl, and brought to pH 3.4. Absorption spectra at temperatures between −0.3°C and

46.3°C were recorded with an Aminco DW-2000 spectrophotometer. The sample was thermostatted with a Lauda K4R waterbath filled with ethanol. The sample temperature was recorded continuously with a PT100 temperature probe. Thermal accuracy was better than 0.1°C. A continuous nitrogen flow was applied to the cuvette holder, to prevent condensation on the outer surface of the cuvette at lower temperatures. The spectra were considered to represent equilibrium conditions when four spectra, measured during a 15-min interval, were identical.

Time-resolved absorption spectroscopy

All time-resolved absorbance measurements were performed with purified PYP, dissolved in 10 mM Tris-HCl at pH 7.5 with or without 3% butanol. The sample was thermostatted with a Lauda waterbath at a sample temperature between 5 and 60°C, which was measured continuously with a PT100 element. Thermal accuracy was better than 0.1°C. The third harmonic of a Nd:YAG laser (DCRA; Quanta-Ray/Spectra Physics) was used either directly for excitation of the sample at 355 nm or was used to pump a pulsed dye laser (PDL2; Quanta-Ray/Spectra-Physics) using Coumarine 440 laser dye to obtain 446-nm flashes. A diffusor was used to eliminate hot spots in the laser beam reaching the sample. The laser energy after the diffusor was typically 0.5 mJ/pulse·cm^2 for the 446-nm light and 5 mJ/pulse·cm^2 for the 355-nm light, resulting in the excitation of, respectively, 10% and 5% of the PYP into the photocycle upon each flash. The delay time between flashes (4 s or more) was chosen to ensure complete relaxation of the sample during this time. The measuring light from a 150-W tungsten halogen lamp was passed through two monochromators, one before and one after the sample, and was detected by a Hamamatsu R456 photomultiplier. The response time of the set-up was 3 μs. The traces were recorded with a Lecroy 99310 recorder at four different time scales to probe the complete time domain that was relevant for the PYP photocycle (0–500 μs, 0–10 ms, 0–200 ms, and 0–2 s), with 2000 data points per trace, and were stored for further analysis. Between 4 and 32 flashes were averaged at each wavelength. Traces were measured at four or more different wavelengths at each temperature. A detailed analysis of the data set of 21 wavelengths at 18°C has been described elsewhere in combination with data obtained on a diode array set-up (Hoff et al., 1994c).

Analysis of the data

The equilibrium measurements as a function of temperature were analyzed with the help of a spectral model (Van Stokkum et al., 1994). The method for the analysis of the kinetic data has been described in detail by Hoff et al. (1994c). It is based on the global analysis approach described by Van Stokkum et al. (1993, 1994). In this method, singular-value decomposition (Henry and Hofrichter, 1992; Malinowski, 1991) is used to determine the number of independent components present in the data set, consisting of a matrix that contains the measured absorbance transients at the different wavelengths. These components are split into left and right singular vectors. The left singular vectors contain information on the concentration of the components as a function of temperature in the equilibrium measurements, or of time in the kinetic experiments, whereas the right singular vectors contain information on the spectral characteristics of the components. For the equilibrium measurements we have analyzed these singular vectors with a two-component model. The first left singular vectors of the kinetic data were analyzed with the programs DISCRETE (Provencher and Vogel, 1980), CONTIN (Provencher, 1982), and FTIKREG (Weese, 1992) to examine the number, value, and amplitude of rate constants present in the data.

The temperature dependence of the equilibrium concentrations of pG and pB_{dark} was analyzed with Eq. 7 and the temperature dependence of the reaction rates with Eq. 13, using the statistical package Splus.

RESULTS

Equilibrium measurements: the thermal denaturation of PYP

PYP is very resistant to thermal denaturation (Meyer et al., 1987), but it can be reversibly denatured by decreasing the pH to below 3.25 (Meyer, 1985). Therefore, we decided to examine the thermal denaturation of PYP at pH 3.4, because we expected that at this pH the thermal transitions in PYP would occur in an experimentally convenient temperature domain. The absorbance band of PYP in the visible part of the spectrum is sensitive to changes in the protein part of the PYP holoenzyme. Denaturing treatments, like heating and lowering of the pH, cause a transition from pG to pB_{dark}, another form of the protein absorbing near 345 nm (Meyer, 1985; Meyer et al., 1987). Decreasing the pH from 7.5 to 3.4 resulted in a loss of 25% of the absorbance at 446 nm at room temperature, with a concomitant increase in absorbance at approximately 350 nm (not shown). In Fig. 1 *a* the spectra of PYP at pH 3.4 are shown at temperatures from −0.3°C to 46.3°C. Increasing the temperature from −0.3°C to 46.3°C resulted in a 53% loss of absorbance at 446 nm, accompanied by an increase in absorbance at 350 nm. At neutral pH the absorbance spectrum of PYP is not significantly affected by such changes in temperature. The difference absorbance spectra with respect to the spectrum at −0.3°C are shown in Fig. 1 *b*. The temperature-induced denaturation process at pH 3.4 cannot be completely described by a two-state model with a ground state pG and a blue-shifted state pB_{dark} (assuming temperature independence of the spectra), as can be concluded from these difference spectra, which show an unexpected fine structure around 470 nm (Fig. 1 *b*). However, the transition is isosbestic at 384 nm, and the cause of the fine structure around 470 nm may well be the temperature dependence of the absorbance spectrum of pG (see Discussion).

To analyze the spectra associated with the thermal denaturation of PYP, a global analysis of the spectra as a function of temperature was performed, assuming a two-state transition (Fig. 1, *c* and *d*). One species was assumed to have the absorbance spectrum of PYP at pH 7.5 (a pure pG spectrum), and the other, pB_{dark}, was modeled with a skewed Gaussian (which was shown to be an adequate description of the spectrum of pB in the photocycle; Hoff et al., 1994c). The spectra in this fit are assumed to be temperature independent. From the constraint that the sum of the concentrations (Fig. 1 *c*, *triangle*) of the two species is constant, the absorbance of pB_{dark} was determined to be at maximum at 354 nm with an extinction coefficient of 0.52, relative to the extinction coefficient of pG at 446 nm. The residuals of this fit resembled the fine structure around 470 nm in the difference spectra in Fig. 1 *b* (not shown). The concentration profiles of pG and pB_{dark} from Fig. 1 *c* were used to calculate the temperature dependence of the equilibrium constant K, describing the equilibrium between pG and pB_{dark}. The temperature dependence of K was analyzed

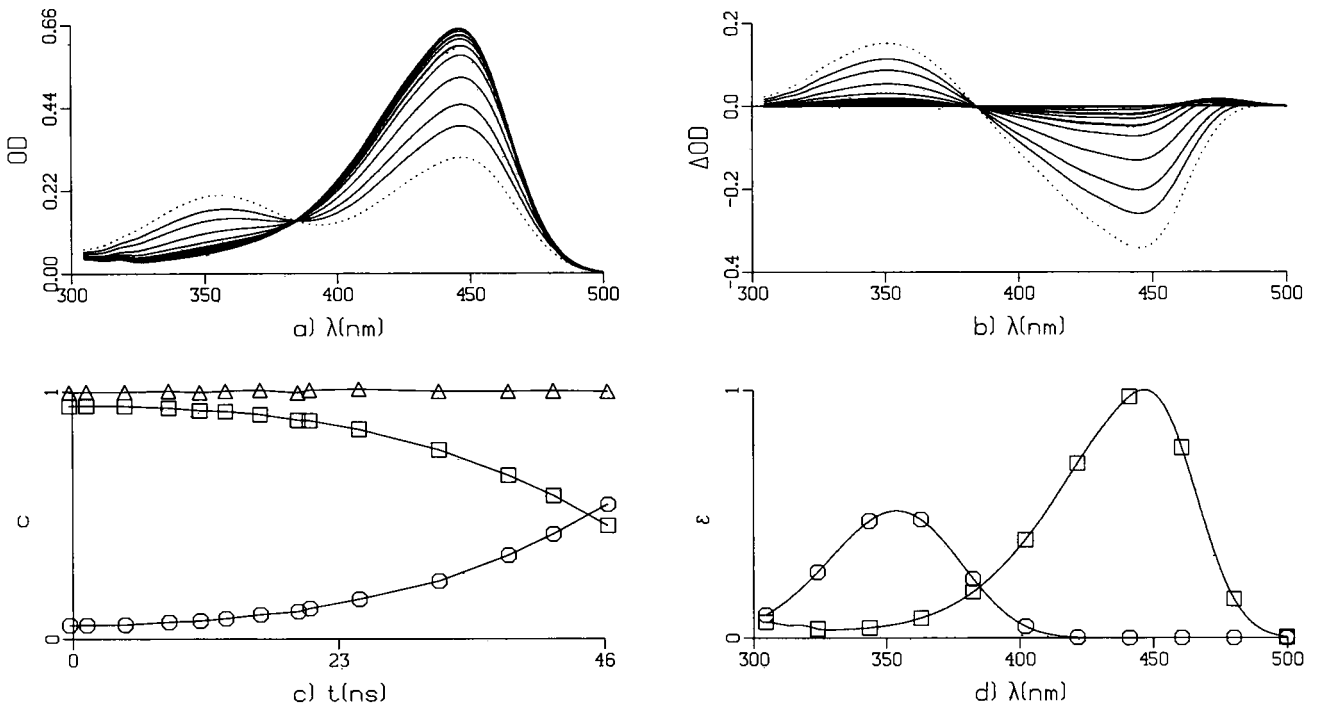

FIGURE 1 Measurement and global analysis of the temperature dependence of the UV-VIS absorbance spectrum of PYP at pH 3.4. The absorbance spectrum of PYP was measured at the following temperatures: −0.3, 1.2, 4.5, 8.3, 11.0, 16.2, 19.5, 24.8, 31.7, 37.7, 41.6, and 46.3°C (*a*). The difference absorbance spectra calculated from *a* with respect to the spectrum at −0.3°C are shown in *b*. The dotted lines indicate the spectrum at 46.3°C. The absorbance spectra shown in *a* were fitted with a model containing two species: pB_{dark}, of which the spectrum was modeled as a skewed Gaussian, and pG, for which we took the spectrum recorded at pH 7.5. The concentration profiles (*c*) and absorbance spectra (*d*) of pG (□) and pB_{dark} (○) were scaled, using the constraint that the sum of the concentrations of these two species in *c* (△) is constant.

using Eq. 7 (Fig. 2). From this fit the thermodynamic parameters that describe the thermal denaturation of PYP were determined (Table 1).

Kinetic measurements: the temperature dependence of the PYP photocycle kinetics

The kinetics of the spectral changes in the PYP photocycle at 18°C have recently been examined in detail (Hoff et al., 1994c). It was shown that both transitions in the PYP photocycle show at least biexponential behavior. The transition from pR to pB is described by two lifetimes of 0.25 ms and 1.2 ms; the relative contribution of these two lifetimes is 60% and 40%, respectively. The last step in the photocycle, the recovery of pG from pB, is only slightly biexponential: it can be described with a decay with a lifetime 0.15 ms with a relative amplitude of 93% and an additional decay with a lifetime of 2 s and a relative amplitude of 7%. A physical interpretation of this biexponential behavior of these processes cannot be provided unambiguously yet.

To examine the temperature dependence of the PYP photocycle kinetics, we performed a separate global analysis of the flash-induced absorbance changes at each temperature studied. Singular value decomposition of the photocycle signals was performed, and the first left singular vectors at the different temperatures resulting from these decompositions are shown in Fig. 3. The advantage of an analysis of the first left singular vector is that data from all wavelengths are combined in this trace, thereby significantly improving the signal-to-noise ratio compared to the analysis of a single wavelength measurement. In Fig. 3 it is clearly visible that the rate of formation of pB from pR monotonically increases with temperature, whereas the rate of its decay (i.e., the pB-to-pG transition) first increases with temperature up to 31.1°C, after which it decreases.

The residuals of a fit, using a photocycle model with two monoexponential transitions, were, like the 18°C measurement (see Hoff et al., 1994c), unsatisfactory for the data measured at the various temperatures reported in this study. We therefore analyzed the number of rate constants needed to describe the photocycle signals at different temperatures. For this purpose we fitted the first left singular vector in two different ways: assuming either discrete rate constants or a distribution of rate constants. Two types of programs were used: 1) the DISCRETE program, which determines the optimal number, value, and amplitude of discrete rate constants needed to fit the data, and 2) the CONTIN and the FTIKREG program, which fit the data to a continuous distribution of rate constants.

The analysis of the data sets at different temperatures with DISCRETE yielded the following results. The slow component, with a lifetime of approximately 2 s, that is present in the signals recorded at 18°C (Hoff et al., 1994c)

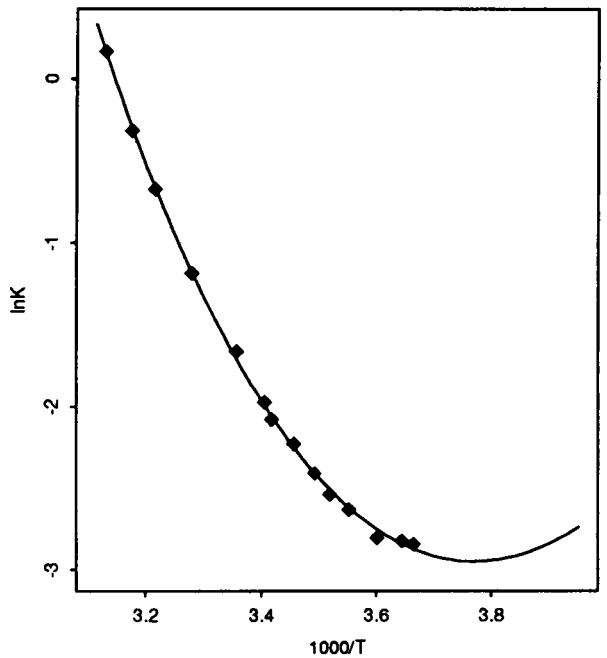

FIGURE 2 Temperature dependence of the equilibrium constant describing the reversible thermal denaturation of PYP. The concentration profiles from Fig. 1 *C* were used to calculate the temperature dependence of equilibrium constant *K*, describing the transition between the pG and pB_{dark} state of PYP. This temperature dependence was fitted using Eq. 7.

was present at all temperatures. The amplitude of this component was approximately 10% of that of the main component describing the pB-to-pG transition. The main component had a lifetime ranging between 143 and 752 ms, depending on temperature. Two rate constants are associated with the pR→pB transition in the temperature domain from 5.3 to 24.3°C. The lifetime of the fastest component decreased from 562 to 98 μs and of the slower component from 4.9 ms to 250 μs, upon a temperature increase from 5.3 to 24.3°C. The relative contribution of the fastest component ranged from 38% to 56% in this range of temperatures. At temperatures above 31.1°C, only a single time constant was required to describe the pR→pB transition, which decreases from 105 to 9.1 μs upon a temperature increase from 34.7 to 60.0°C. However, global analysis of an elaborate data set at 18°C has shown that only two spectrally distinct intermediates are involved in the photocycle (Hoff et al., 1994c). Because it is impossible to find more rate constants than the number of intermediates involved in the process, this means that the additional rate constants found for the PYP photocycle must be attributed to intermediates that have the same spectral but different kinetic properties.

TABLE 1 Thermodynamic parameters of the equilibrium between the pG and pB_{dark} form of PYP at 298 K and pH 3.4

ΔS (J/mol · K)	ΔH (kJ/mol)	ΔG (kJ/mol)	ΔC_p (kJ/mol · K)
161 (1.4)	52.1 (0.4)	4.2 (3.0)	1.59 (0.06)

The values in parentheses are the standard deviations in the thermodynamic parameter, according to the linear least-squares fit of the equilibrium constants at the various temperatures with Eq. 7 (see Fig. 2).

To characterize the kinetic heterogeneity in the PYP photocycle, we analyzed the data, assuming a continuous distribution of rate constants. Because both rise time and a decay time constants are present in the data, both negative and positive amplitudes will occur in the fit, and the nonnegative amplitude constraint, which normally regularizes a fit with a distribution of exponentials, cannot be used. Without this constraint, an analysis with a continuous distribution of rate constants can easily lead to oscillations in the outcome. With the two programs used, the automatically chosen regularization parameter for smoothing of the distribution was rather small, resulting in a distribution with many peaks and troughs. We therefore decided to fix the regularization parameter at a larger value, which resulted in a smooth distribution with only a few peaks and troughs, with the residuals showing little systematic deviation. In Fig. 4 the results of this analysis with a continuous distribution of rate constants are shown for the different temperatures. The troughs (*hatched*) are associated with the pR-to-pB transition, and the peak (*dotted*) describes the major part of the pB-to-pG transition. At low temperatures, two distinct features are associated with the pR-to-pB transition. Upon an increase in temperature, this pattern changes in a gradual manner to a single distributed transition, because, as expected on the basis of previous results, at high temperature this process can be described satisfactorily with a single rate constant. This analysis indicates that below approximately 24.3°C at least two distinct forms of pR exist that are not in equilibrium.

Distribution analyses, in which less smooth results were allowed, resulted in a similar overall outcome, but with more oscillations in the distribution and an even more distinct separation of the two troughs associated with the pR-to-pB transition. We have also tried to fit these data with two broad Gaussian-shaped distributions, for the pR-to-pB and pB-to-pG transitions, respectively (results not shown). This resulted in unacceptable residuals at temperatures below 24.3°C.

The effect of butanol on the photocycle kinetics at a single wavelength and a number of temperatures was also examined to investigate the thermodynamic basis for the effect of this compound on the kinetics of the transitions in the photocycle of PYP. In the presence of 3% (v/v) butanol, the photocycle could be described with two rate constants at all temperatures investigated (data not shown). However, it may well be that a higher signal-to-noise ratio will reveal more rate constants.

The multiexponential behavior of the PYP photocycle transitions hampered a straightforward thermodynamic interpretation of the temperature dependence of the kinetics of these processes. Because more than 90% of the last step in the photocycle can be described by a monoexponential decay, we neglected the remaining process of small ampli-

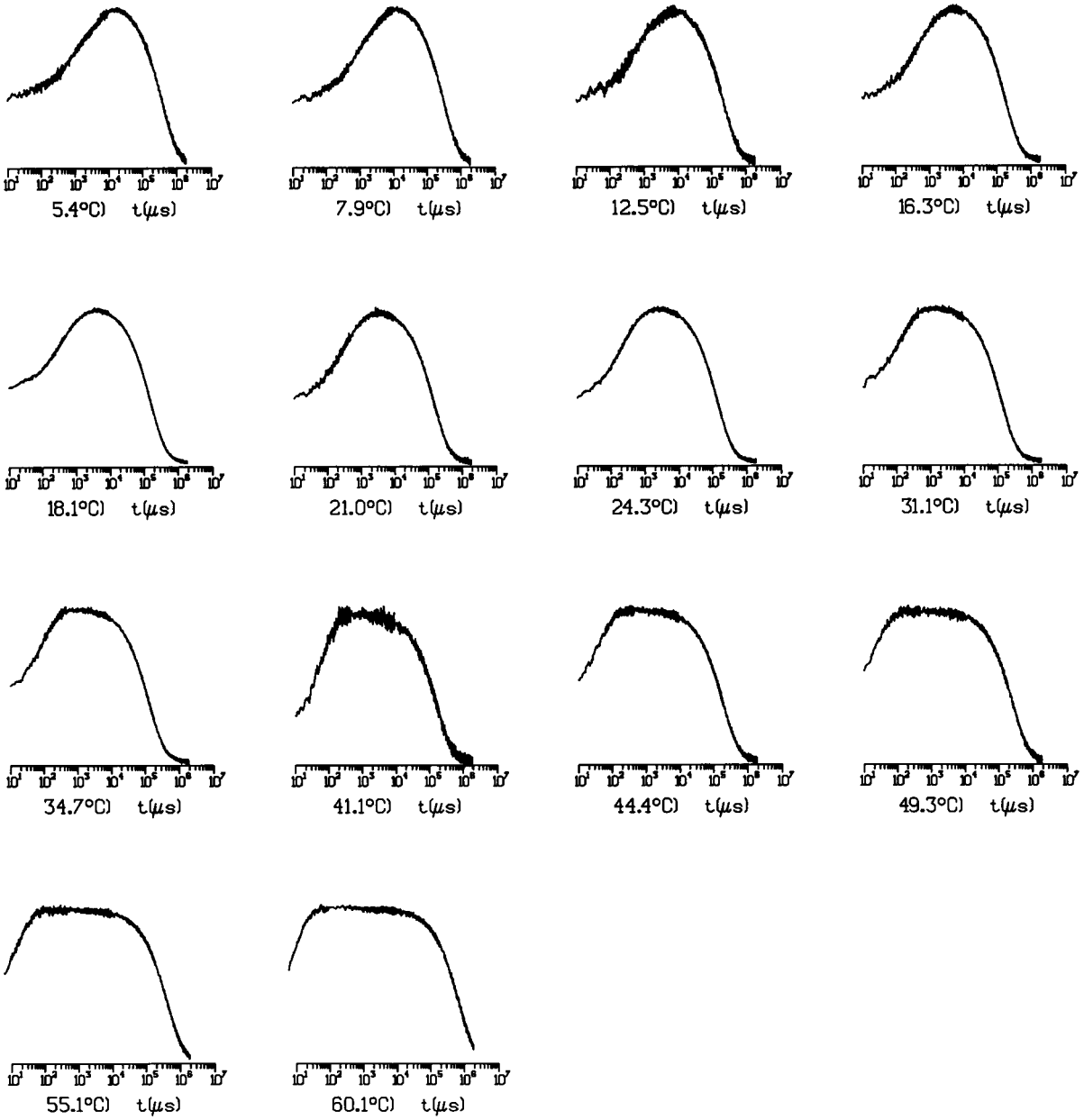

FIGURE 3 Temperature dependence of the photocycle transients of PYP. Time-resolved absorbance difference traces were recorded at a number of different wavelengths and at a number of different temperatures between 5 and 60°C. Data from multiple wavelengths were used to calculate the first left singular vector, which summarizes the kinetic information. This first left singular vector is depicted at different temperatures indicated at the abscissa.

tude. The problems resulting from the biexponential behavior of the pR-to-pB transition are dealt with below.

The pB-to-pG transition

Fig. 5 shows the temperature dependence of the activation equilibrium constant $K^{\#}$ (which is related to the reaction rate constant k through Eq. 12) of the component with the dominant amplitude in the pB-to-pG transition in 10 mM Tris-HCl, with and without 3% butanol (v/v), as calculated with DISCRETE from the left singular values shown in Fig. 3. These results show that under both conditions, a characteristic curvature of the temperature dependence of $K^{\#}$ is found.

Analysis of the data with Eq. 13 yields the thermodynamic activation parameters describing this transition. The results of the fits with equation 13 are presented in Table 2. The standard error in the estimated thermodynamic parameters is satisfactory. With these parameters the temperature dependence of $\Delta H_i^{\#}$, $\Delta S_i^{\#}$, and $\Delta G_i^{\#}$ can be calculated according to activation thermodynamic analogues of Eqs. 2, 3, and 4 (Fig. 6). Analysis of the pB-to-pG transition in a data set with 355-nm excitation and a lower signal-to-noise ratio (not shown), which was analyzed using two monoexponen-

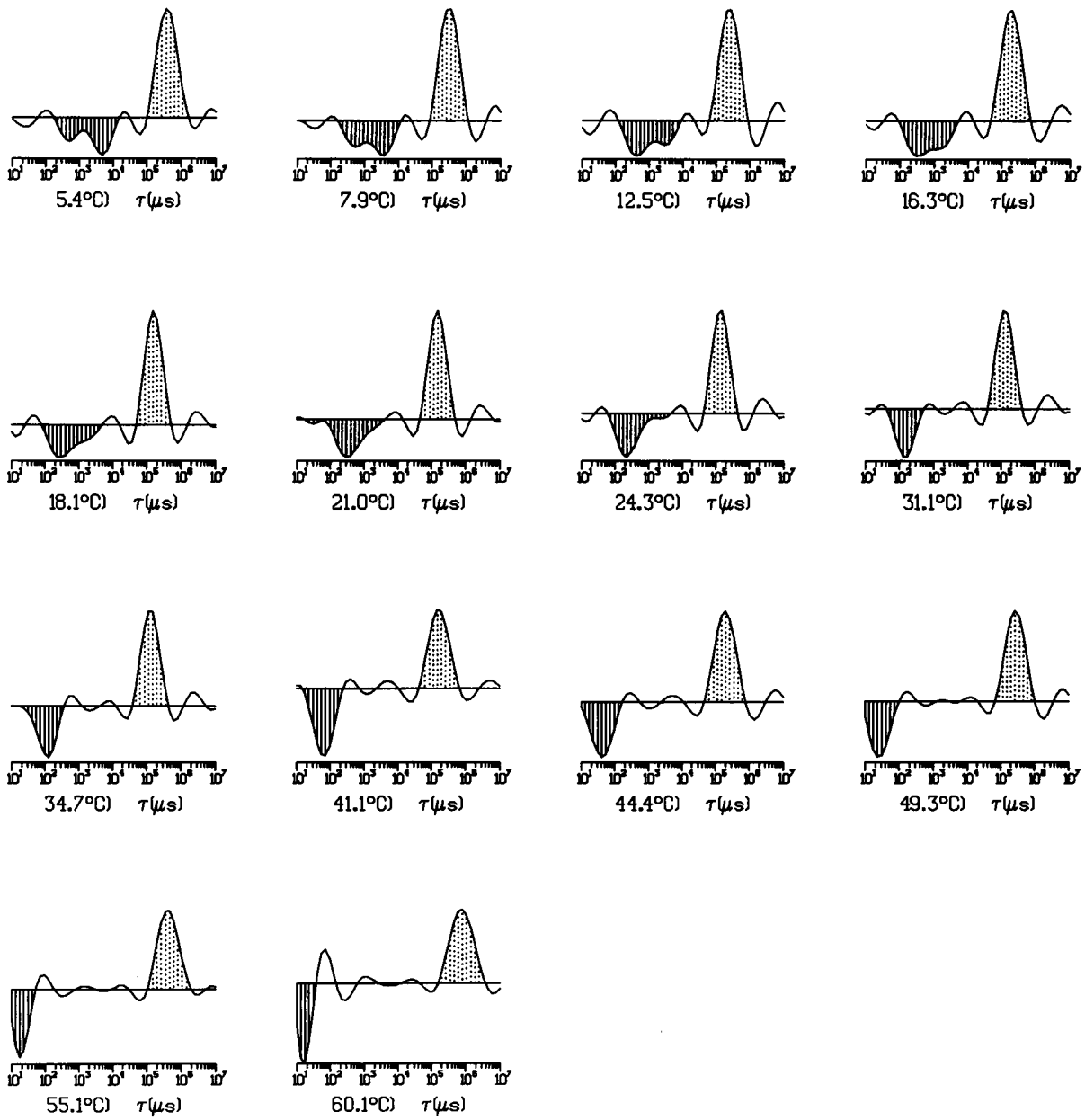

FIGURE 4 Analysis of the PYP photocycle kinetics with a continuous distribution of rate constants as a function of temperature. The first left singular vectors shown in Fig. 3 were fitted with a continuous distribution of rate constants, and the results for the various temperatures are depicted. The rise associated with the pR to pB transition is indicated by the negative (*hatched*) area, whereas the decay associated with the pB to pG transition is indicated by the positive (*dotted*) area.

tial decays, yielded similar thermodynamic parameters (see Table 2). Note that at 298 K the free energy of activation is almost entirely determined by the activation entropy.

The pR-to-pB transition

In Fig. 7 *A* the temperature dependence of the pR-to-pB transition of PYP in 10 mM Tris-HCl and 10 mM Tris-HCl with 3% butanol is shown and analyzed assuming monoexponential kinetics. These absorbance traces were obtained in experiments using excitation of the PYP photocycle with 355-nm laser pulses. The deviation of the linearity of the temperature dependence is small. As a result, analysis of these data with Eq. 13 leads to small estimated heat capacity changes of activation.

The data set depicted in Fig. 3, which has a higher signal-to-noise ratio, could not be satisfactorily described with one rate constant at lower temperatures (see above), complicating its thermodynamic analysis. We have examined the data above 31.1°C and below 24.3°C as two different domains, one in which the pR→pB transition is biexponential and one in which it is monoexponential (Fig.

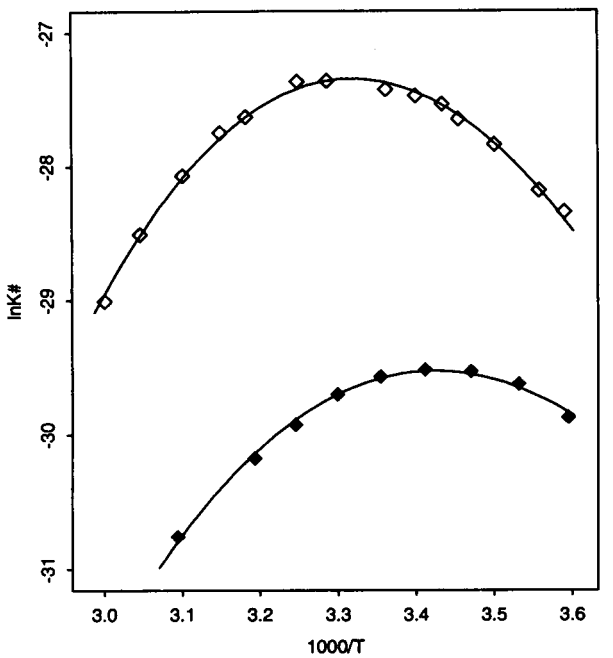

FIGURE 5 Thermodynamic analysis of the pB to pG transition in the PYP photocycle. The activation equilibrium constant $K^{\#}$, calculated from the rate constant k and describing more than 90% of the pB-to-pG transition, is shown as a function of temperature. This temperature dependence was fitted using Eq. 13. Empty diamonds represent data obtained with PYP dissolved in 10 mM Tris-HCl, pH 7.5, and filled diamonds indicate data obtained in the same buffer but in the presence of 3% (v/v) butanol.

7 *B*). The temperature dependence of these rate constants was analyzed separately by using Eq. 13, and for all three cases the results are given in Table 3. It should be noted that because of the smaller temperature range for these fits, the outcome is less reliable, which also follows from the large standard errors. Therefore, at this moment the best estimate of the heat capacity change is the value of 0.35 $kJ \cdot mol^{-1} \cdot K^{-1}$, obtained in a fit in which a broader temperature range was analyzed (Fig. 7 *A*). This is much smaller than the value, with opposite sign, of -2.7 $kJ \cdot mol^{-1} \cdot K^{-1}$ found for the pB-to-pG transition (Table 2).

DISCUSSION

Reversible thermal denaturation of PYP: the pG→pB_{dark} equilibrium

At neutral pH PYP shows a remarkable resistance against heat denaturation (Meyer et al., 1987). Under acidic conditions, however, it is destabilized. This has enabled us to study the reversible thermal denaturation of PYP. In the difference spectra associated with this process, unexpected features around 470 nm were observed (Fig. 1 *b*). This was also clear from the residuals of a global analysis of the absorbance spectra, using a two-component model (not shown). Most likely, this phenomenon can be explained by a temperature dependence of the absorbance spectrum of pG, which may be due to the coupling of the optical transition to low-frequency phonons. Then the distribution over the different "phonon substates" is affected by temperature. The higher energy states become increasingly populated with increasing temperature, resulting in a red shift and broadening of the absorbance band (Pullerits et al., 1994). The changes in the absorbance spectra that occur when PYP is cooled to 77 K (Hoff et al., 1994c) are reminiscent of the spectra shown in Fig. 1 *a* and probably have the same origin.

In spite of this complication, we were able to obtain a thermodynamic description of the denaturation process using a two-state model for the conversion of the native state pG into pB_{dark} (Table 1). The temperature dependence of the equilibrium constant describing the thermal denaturation of PYP showed a curvature that is very characteristic (Privalov, 1979; Pace, 1990) for protein denaturation processes (Fig. 2). The heat capacity change, 1.6 $kJ \cdot mol^{-1} \cdot K^{-1}$, is smaller than the heat capacity changes that have been reported for the unfolding reaction of small water-soluble proteins. However, some care should be taken in the interpretation of the exact value of this parameter, because mainly data were obtained in the declining part of the curve (Fig. 2). The average value of the heat capacity change for this process, measured by scanning microcalorimetry, is 7.5 $kJ \cdot mol^{-1} \cdot K^{-1}$, and the smallest value reported is 4.6 $kJ \cdot mol^{-1} \cdot K^{-1}$. The smallest heat capacity change per mole of amino acid is 43 $J \cdot mol^{-1} \cdot K^{-1}$ (Privalov, 1988). For the transition in PYP between pG and pB_{dark} this equals 12 $J \cdot mol^{-1} \cdot K^{-1}$. This indicates that pB_{dark} is not in a totally unfolded random coil conformation, but has a structure in which some of the hydrophobic amino acids are still buried within the protein interior. This conclusion is supported by circular dichroism measurements (Hoff et al., unpublished results). Interestingly, a small heat capacity change has also been reported for the transition between the native and the molten globule states of apolactalbumin (Xie et al., 1991). For this protein (123 amino acids) it was found that the ΔC_p occurring during the transition from the native to molten globule state is 1.4 $kJ \cdot mol^{-1} \cdot K^{-1}$, whereas the ΔC_p for the transition from the molten globule to the unfolded state is significantly larger: 7.6 $kJ \cdot mol^{-1} \cdot K^{-1}$.

Protein folding thermodynamics applied to the PYP photocycle

An observation concerning PYP that was left unexplained in the literature is the unusual non-Arrhenius behavior of its photocycle kinetics (Meyer et al., 1989). Because it was reported that solvent hydrophobicity has a marked effect on photocycle kinetics at room temperature (Meyer et al., 1989; see Introduction), we examined the possibility that for the description of this light-induced enzymatic process a thermodynamic description incorporating changes in heat capacity, which was developed for the description of protein de/renaturation processes, is required. Therefore, we applied the thermodynamic model described above to the two

TABLE 2 Activation thermodynamic parameters of the transition from pB to pG without and with the addition of 3% (v/v) butanol at 298 K

	$\Delta S^{\#}$ (kJ/mol · K)	$\Delta H^{\#}$ (kJ/mol)	$\Delta G^{\#}$ (kJ/mol)	$\Delta C_p^{\#}$ (kJ/mol · K)
Main component of biexponential fit	−196 (2)	9.2 (0.6)	67.77 (0.04)	−2.73 (0.06)
Monoexponential fit*	−210 (3)	5.5 (0.9)	68.12 (0.06)	−2.81 (0.1)
Addition of 3% (v/v) butanol*	−288 (2)	−12.7 (0.6)	73.25 (0.04)	−2.13 (0.1)

For all experiments PYP was dissolved in 10 mM Tris-HCl. The values in parentheses are the standard deviations in the thermodynamic parameters according to the linear least-squares fit of the rate constants at the various temperatures with Eq. 13. The fit of the rate constants is presented in Fig. 6 for the experiments in the first and third rows.
*The excitation wavelength is 355 nm.

transitions occurring in the PYP photocycle. A number of arguments support the appropriateness of this model.

First, the curved temperature dependence of the kinetics of the last step in the PYP photocycle can be fitted very satisfactorily with the model used (see Fig. 5). Second, the value of $\Delta C_p^{\#}$ calculated from this fit is very similar to the values reported for protein (un)folding processes (see below). Therefore, the temperature dependence of the kinetics of the last step of the PYP photocycle can be quantitatively explained with the single assumption that a $\Delta C_p^{\#}$ occurs during the photocycle. This assumption follows very naturally from the observation that viscosity and hydrophobicity markedly affect photocycle kinetics, indicating that a conformational change occurs during the photocycle, during which PYP exposes hydrophobic sites to the solvent (Meyer et al., 1989). The assumption in the model that the changes in activation heat capacity are constant with temperature allows a good fit of the data to the model over the whole temperature range studied. Although a detailed analysis has shown that the ΔC_p associated with protein folding events may be sligthly dependent on temperature (Privalov and Makhatadze, 1990), satisfactory results have been obtained in the analysis of the (un)folding thermodynamics of a large number of proteins, assuming that this parameter is constant with temperature (Privalov, 1988).

Although a large number of proteins have been studied with respect to their equilibrium thermodynamic parameters of thermal denaturation (see Privalov, 1988), we are aware of only three studies of the dependence of the kinetics of protein (un)folding on temperature: studies on hen egg-white lysozyme (129 residues; Segawa and Sugihara, 1984), a mutant form of phage T4 lysozyme (164 residues; Chen et al., 1989), and chymotrypsin inhibitor (83 residues; Jackson and Fehrst, 1991). The values for $\Delta C_{p,unfolding}^{\#}$ that were reported for these three proteins were 0, 2.3, and 0.8 $kJ \cdot mol^{-1} \cdot K^{-1}$, respectively, where the latter value was smaller than the detection limit in the experiments of Jackson and Fehrst, but could be calculated by the incorporation of equilibrium data. The values found for the $\Delta C_{p,folding}^{\#}$ were significantly larger: −6.7, −8.8, and −2.5 $kJ \cdot mol^{-1} \cdot K^{-1}$, respectively. The values for the $\Delta C_p^{\#}$ associated with the pR-to-pB (approximately 0.35 $kJ \cdot mol^{-1} \cdot K^{-1}$) and the pB-to-pG transitions (−2.8 $kJ \cdot mol^{-1} \cdot K^{-1}$) in PYP compare well with these data on protein (un)folding: the first photocycle step resembles a protein unfolding event, whereas the latter involves protein refolding.

An interpretation of the apparently general phenomenon that unfolding reactions are accompanied by a significantly smaller $\Delta C_p^{\#}$ than refolding reactions, in terms of molecular structure, is that the transition states of both protein (un)folding reactions and of the PYP photocycle transients ($pR^{\#}$ and $pB^{\#}$) are rather compact, keeping most buried hydrophobic residues shielded from the solvent. This seems to be a general characteristic of the activated complex that occurs during protein folding processes (see Creighton, 1992).

The effect of butanol on the photocycle

We have found that the $\Delta C_p^{\#}$ of the pB-to-pG transition is affected by the addition of 3% (v/v) butanol: its value increases from −2.8 $kJ \cdot mol^{-1} \cdot K^{-1}$ to −2.1 $kJ \cdot mol^{-1} \cdot K^{-1}$. This resembles the results of measurements on egg-white lysozyme, for which the addition of 3.9 M propyl alcohol increases the $\Delta C_{p,folding}^{\#}$ from −6.7 to −4.0 $kJ \cdot mol^{-1} \cdot K^{-1}$ (Segawa and Sugihara, 1984).

The addition of butanol (or other hydrophobicity-increasing organic solvents) causes the pR-to-pB transition to accelerate and the pB-to-pG transition to decelerate. Fig. 6 shows that the deceleration of the pB-to-pG transition by butanol at room temperature is caused by an increase in activation free energy. In the temperature domain studied (278 to 333 K), both the activation enthalpy and activation entropy are lower in 10 mM Tris-HCl with 3% (v/v) butanol, than in the same buffer without butanol. Consequently, the enthalpy effect of butanol lowers the activation free energy, whereas the entropy effect of butanol increases the activation free energy. The net increase in activation free energy is therefore established by the dominating entropy effect of butanol on the activation free energy. The molecular interpretation of these results remains to be established.

A thermodynamic model of the PYP photocycle

The data that are now available on the thermodynamics of PYP allow the construction of a complete, although partly speculative, model for the energetics of the PYP photocycle (Fig. 8). In Fig. 8 *B* the free energy content of the different

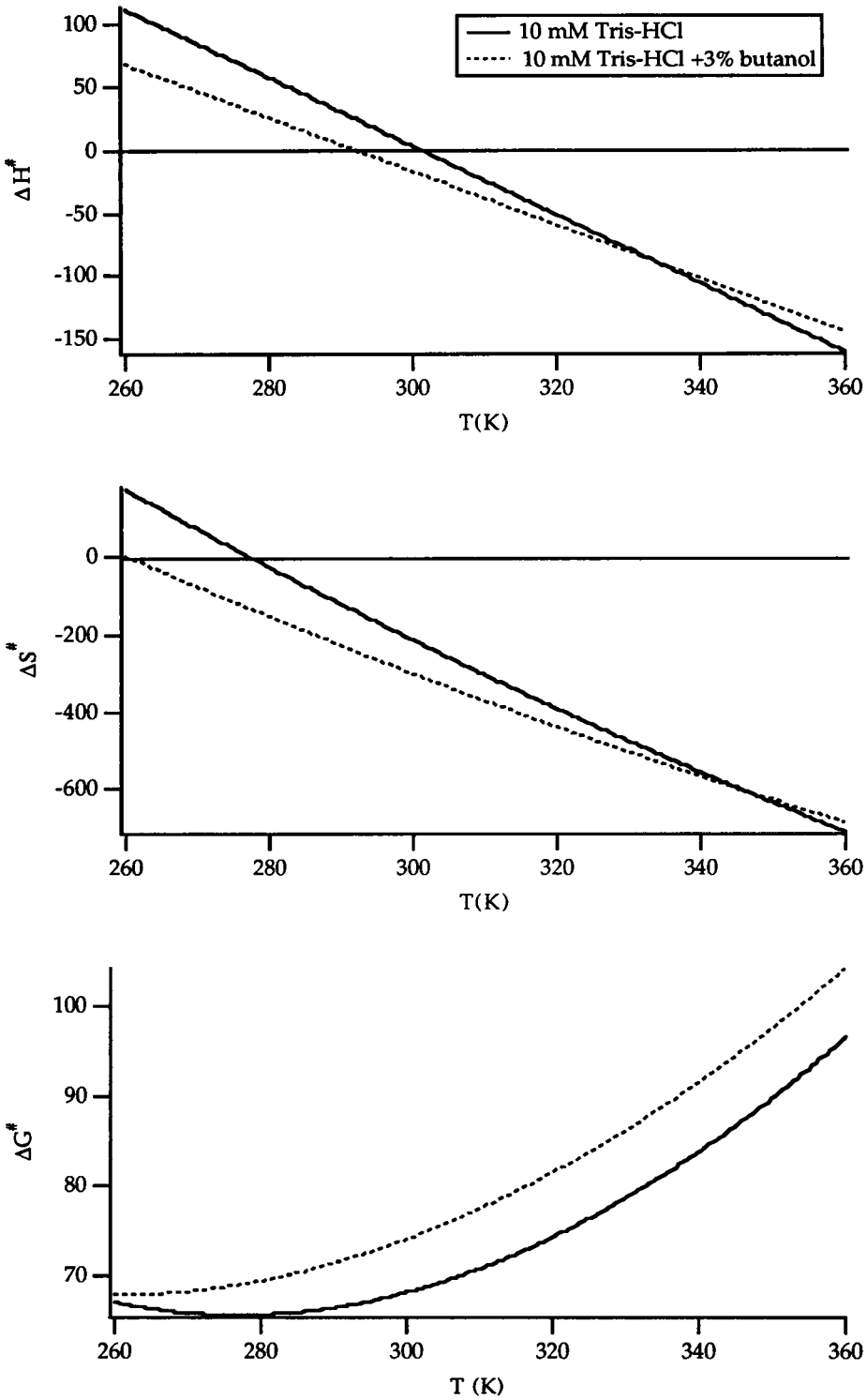

FIGURE 6 Temperature dependence of the thermodynamic activation parameters describing the pB-to-pG transition. The temperature dependence of the thermodynamic activation parameters describing the pB to pG transition was calculated from the coefficients presented in Table 2, using the transition state analogs of Eqs. 3, 4, and 6. Solid lines indicate data obtained with PYP dissolved in 10 mM Tris-HCl, pH 7.5, and dashed lines indicate data obtained in the same buffer, but in the presence of 3% (v/v) butanol.

photocycle intermediates is depicted, as calculated at 25°C. It should be realized that, because of the occurrence of changes in (activation) heat capacity, the scheme depicted in Fig. 8 *B* has a complex temperature dependence.

The energy content of the primary excited state on the S_1 energy surface (formed by the absorption of a photon) can be derived from the spectral position of the 0–0 transition, which is near 469 nm, i.e., 255 kJ/mol (Meyer et al., 1991). It is still unknown whether an energy barrier exists on this energy surface, as suggested by low temperature measure ments (Hoff et al., 1992). Through internal conversion this intermediate returns to the S_0 surface, but the protein is now in the pR state. We have recently determined the energy content of pR with laser-induced optoacoustic calorimetry experiments (Van Brederode et al., 1995). The value depicted in Fig. 8 *B* for this transition is based on these

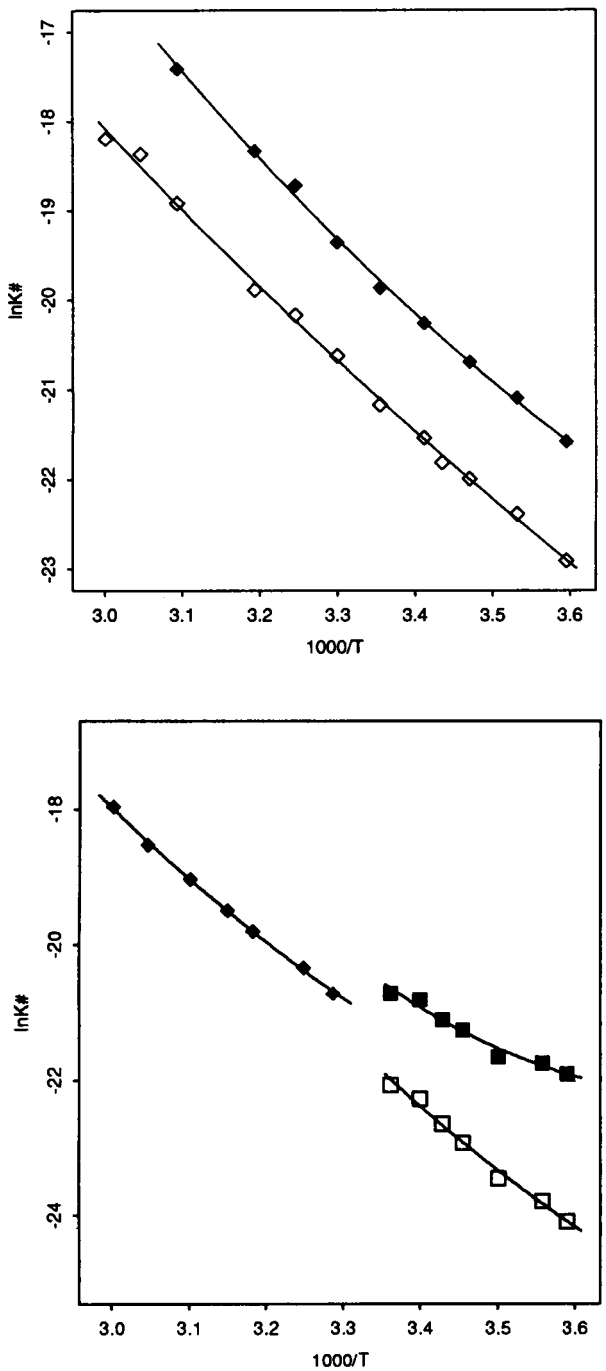

FIGURE 7 Thermodynamic analysis of the pR to pB transition in the PYP photocycle. The activation equilibrium constant $K^{\#}$, calculated from the rate constant k describing the pR-to-pB transition, is shown as a function of temperature. (*A*) Temperature dependence of the activation equilibrium constant $K^{\#}$, calculated from the rate constant k upon description of the pR-to-pB transition as a monoexponential decay. Open boxes indicate data obtained with PYP dissolved in 10 mM Tris-HCl (pH = 7.5), and filled boxes are the data obtained in the same buffer in the presence of 3% butanol. The temperature dependence of these rate constants was fitted using Eq. 13. (*B*) Temperature dependence of activation equilibrium constant $K^{\#}$ calculated from the rate constant k, using a biexponential decay to describe this transition when necessary. Below 24.3°C, two rate constants were needed to describe the pR-to-pB transition in 10 mM Tris-HCl (pH 7.5), whereas above this temperature one rate constant was sufficient. This resulted in the three curves shown.

experiments. The energy barriers that have to be crossed in the transition from pR to pB via $pR^{\#}$ and from pB to pG via $pB^{\#}$ have been described in detail above.

This leaves the value of the ΔG between pB and pG. We have not directly determined this value, but an estimation of this value can be obtained from equilibrium measurements from literature between pB_{dark} and pG. The assumption that pB and pB_{dark} are thermodynamically equivalent seems reasonable, because the spectra of pB and pB_{dark} are reminiscent. There are a number of estimates for the ΔG between pB and pG. First, Meyer et al. (1987) have studied the urea-induced denaturation of PYP and have reported a value of 45 kJ/mol. Second, a calculation based on the acid denaturation, which uses the midpoint of denaturation at a pH of approximately 2.7 (Meyer, 1985), yields a value of 15 kJ/mol, when it is assumed that the protonation of a single amino acid in PYP causes the denaturation process. An intermediate value of 30 kJ/mol has been used in Fig. 8 *B*. The data presented in Fig. 1 *a* yield a much lower value of 4.2 kJ/mol. This, of course, must be explained by the fact that the protein is destabilized at pH 3.4.

Kinetic heterogeneity in the PYP photocycle

The kinetics of the two slowest transients of the PYP photocycle cannot be described by two rate constants. This conclusion was reached on the basis of an extensive analysis of a large data set of transient absorbance measurements (Hoff et al., 1994c) and is confirmed by the results described here (Fig. 4). The largest part (approximately 90%) of the transition from pB to pG can be described, however, by a single rate constant. The situation is more complex for the case of the transition from pB to pR. At lower temperatures, two distinct rates are associated with this process. However, at increasing temperatures the contribution of the slower component diminishes, until it has completely disappeared at approximately 31.1°C. A possible interpretation of these results is that two distinct forms of pR (pR_{slow} and pR_{fast}) are at equilibrium. At lower temperatures the equilibration of these two species is slow as compared to their decay to pB, whereas at higher temperatures the reverse is true. Therefore, at higher temperatures all molecules reach pB via pR_{fast}, and at lower temperatures both forms of pR decay to pB. Further experimentation is needed to establish the existence of two different forms of pR, e.g., by double flash experiments.

Protein conformational changes in the PYP photocycle

What is the nature of the conformational changes occurring during the PYP photocycle? Although a complete answer to this question in structural terms will have to await the determination of the high-resolution structure of photocycle intermediates by crystallographic and/or nuclear magnetic resonance spectroscopic studies, a partial answer can be deduced from the results described above. It should be noted that the transients in the photocycle of PYP are directly

TABLE 3 Thermodynamic parameters of the transition form pR to pB without and with the addition of 3% (v/v) butanol at 298 K

	$\Delta S^{\#}$ (J/mol · K)	$\Delta H^{\#}$ (kJ/mol)	$\Delta G^{\#}$ (kJ/mol)	$\Delta C_p^{\#}$ (kJ/mol · K)
Below 24.3°C, fast component.¶	51 (53)	66 (16)	50.9 (0.2)	1.9 (1.5)
Below 24.3°C, slow component.¶	114 (49)	88 (15)	54.3 (0.2)	1.2 (1.3)
Above 24.3°C¶	25 (20)	60 (6)	52.5 (0.2)	0.92 (0.3)
Monoexponential fit.*§	44 (4)	65 (1.3)	52.3 (0.08)	0.35 (0.14)
Addition of 3% (v/v) butanol, monoexponential fit.*§	65 (4)	68 (1.2)	49.0 (0.1)	0.70 (0.2)

For all experiments PYP was dissolved in 10 mM Tris-HCl. The values in parentheses are the standard deviations in the thermodynamic parameters according to the linear least-squares fit of the rate constants at the various temperatures with Eq. 13.

*The excitation wavelength of the experiments is 355 nm.

§The fit of the rate constants is presented in Fig. 7 *A*.

¶The fit of the rate constant is presented in Fig. 7 *B*.

comparable to (conformational) intermediates of an enzyme during catalysis. Catalysis by PYP during the photocycle applies to at least two aspects: 1) the transient formation of the signaling state of this photoreceptor (see Meyer et al., 1989; Sprenger et al., 1993) and 2) the reisomerization of the chromophore. This latter point has not yet been proved, but there is every reason to suppose that light induces *trans* to *cis* isomerization in the *p*-coumaric acid chromophore (see Hoff et al., 1994a). Consequently, the apoprotein of PYP catalyzes the reisomerization of the chromophore to the *trans* isomeric configuration in the dark. The evidence obtained so far indicates that the apoprotein considerably decreases the kinetic barrier for reisomerization. For the free chromophore the activation free energy for thermal isomerization is typically 160 kJ/mol at room temperature (Ross and Blanck, 1971), whereas for the pB-to-pG transition we found a value of 68 kJ/mol.

Because pR is formed within 1 ns, it is unlikely that major protein conformational changes have already occurred during the formation of this intermediate, implying that the ΔC_p associated with pR formation is probably negligible (see Fig. 8 *C*). The transition from pR to pB occurs on a sub-millisecond time scale, and it seems unlikely that the protein is completely unfolded in this step, because it is part of the physiological catalytic cycle of the protein. The value of $-2.8\ \text{kJ} \cdot \text{mol}^{-1} \cdot \text{K}^{-1}$ implies that approximately 40 of the 125 amino acids in PYP are involved in the pB-to-pB$^{\#}$ transition, exposing approximately 50 Å^2 of hydrophobic surface area to the aqueous solvent (Privalov and Makhatadze, 1990).

The values found for the $\Delta C_p^{\#}$ associated with the PYP photocycle compare well with those reported for egg-white lysozyme (Segawa and Sugihara, 1984), T4 lysozyme (Chen et al., 1989), and chymotrypsin inhibitor (Jackson and Fehrst, 1991) and show that the pR-to-pB transition is thermodynamically equivalent to a protein unfolding reaction, whereas the pB-to-pG transition strongly resembles a protein refolding event. This is remarkable, because we have studied not the kinetics of the unfolding or refolding of a protein after thermal denaturation, but rather the kinetics of the transients in the catalytic cycle of a photoreceptor molecule. Apparently, the features of the transition states pR$^{\#}$ and pB$^{\#}$ in the PYP photocycle are similar to those of the transition state for the (un)folding of small globular water-soluble proteins. Because PYP is the photoreceptor for a negative phototactic response (Sprenger et al., 1993), this result indicates that the large protein conformational change occurring in the PYP photocycle may well be the basis of the mechanism of signal transduction of this photoreceptor protein.

The results reported here show that the processes occurring in the PYP photocycle are thermodynamically equivalent to protein unfolding and refolding events. This does not necessarily imply that these processes are also mechanistically related. However, based on the analysis of both equilibrium and kinetic data as a function of pH and temperature, we have found that strong parallels exits between reversible acid and thermal denaturation of PYP and the transient formation of pB in the PYP photocycle (Hoff et al., manuscript in preparation). The structures of pB and pB_{dark} remain to be determined by x-ray (see Ng et al., 1995) and/or nuclear magnetic resonance methods.

Protein conformational changes in prokaryotic photoreceptor molecules have been inferred for both sensory rhodopsin I and sensory rhodopsin II from *Halobacterium salinarium* (Spudich and Bogomolni, 1988) and have been proposed to be essential for the signaling mechanism of these photoreceptors (Yan et al., 1991a,b). In the case of the light-driven proton pump bacteriorhodopsin, isolated from the same organism, the occurrence of photocycle-associated protein conformational changes has been shown directly (Subramaniam et al., 1993). For eukaryotic photoreceptors conformational changes have been shown to take place in plant phytochromes (Wells et al., 1994; Yamamoto, 1993; Mizutani et al., 1993) and animal rhodopsins (Toossi et al., 1993; Resek et al., 1993; Rath et al., 1993). However, in none of these proteins have changes in heat capacity been reported to occur, whereas this possibility has been specifically investigated for bacteriorhodopsin (Váró and Lanyi, 1991). This may be due to the fact that the retinal proteins are mainly located in the hydrophobic environment of the cytoplasmic membrane and therefore have less extensive protein-water contacts.

CONCLUSIONS

We have shown that a thermodynamic model, developed to describe the thermodynamics of the denaturation of small water-soluble proteins, is also applicable to PYP. The model describes very well both the equilibrium data on the thermal

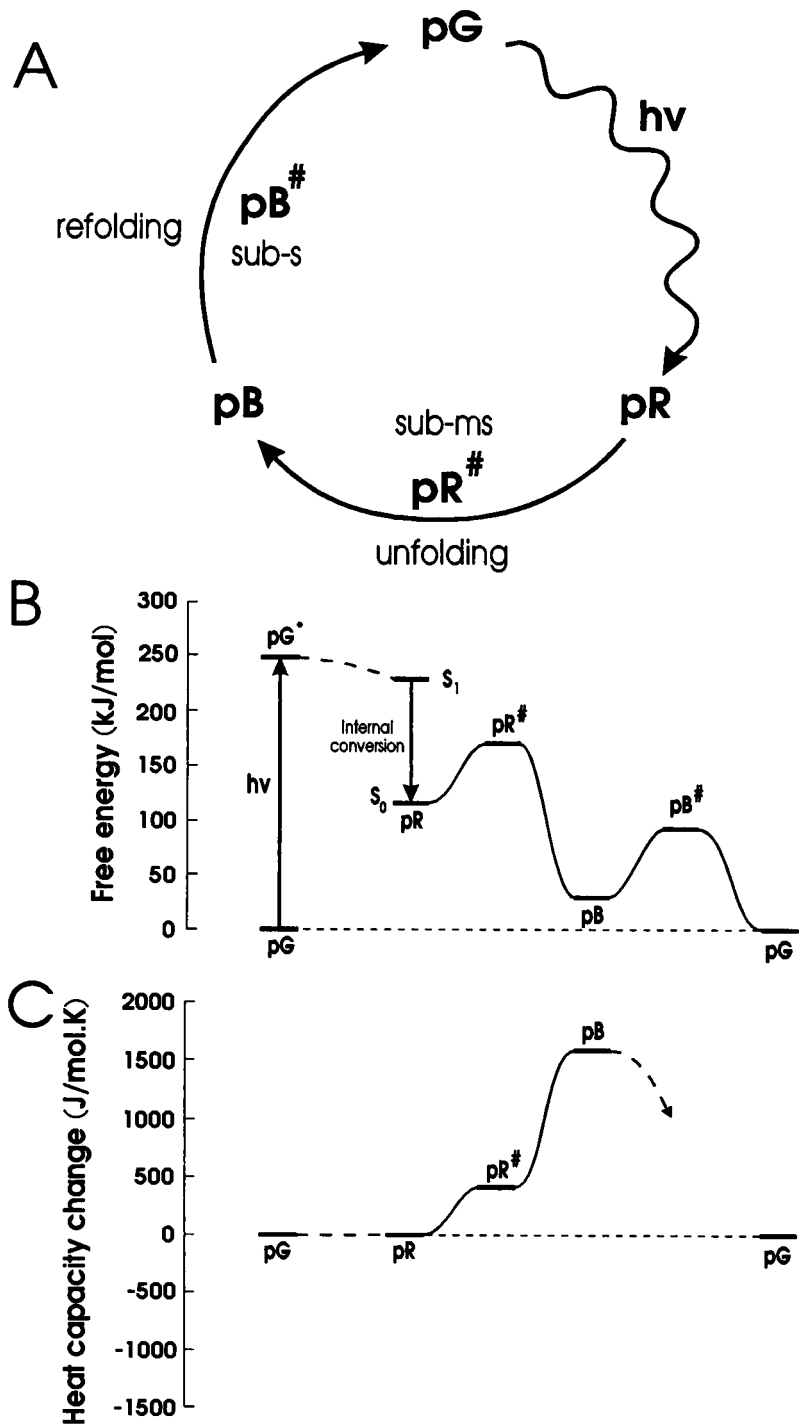

FIGURE 8 Schematic summary of the PYP photocycle and its thermodynamics. (*A*) Schematic representation of the intermediates and activated states in the PYP photocycle. The wavy line indicates the primary light reaction. (*B*) Free energy levels of the different intermediates of the photocycle at 25°C. (*C*) Changes in heat capacity, occuring during the photocycle. The dotted line indicates the uncertainty in the experimentally determined values for the relative values of the heat capacities of pB, pB#, and pG.

denaturation and the kinetic data on the light-induced catalytic cycle of this photoreceptor protein. The thermodynamic parameters determined are comparable to those reported for the re/denaturation of other proteins. A phenomenon that requires further investigation is the physical basis for the multiexponential behavior of two transitions in the PYP photocycle.

A major difference between the study reported here and the data available from the literature is that our kinetic measurements do not concern the denaturation or renaturation of a protein, but instead describe the transitions in the catalytic cycle of a signal-transferring photoreceptor protein performing its physiological function. Therefore, our data bear not only on the physical-chemical problem of protein folding, but also on the mechanism of enzyme catalysis. The resemblance between the PYP photocycle transitions and protein folding processes can be rationalized, because the protein functions as a (water-soluble) photoreceptor, i.e.,

transducing a light signal into a protein conformational change that forms the physiological signal (the signaling state), which causes the bacterial cell to respond to light stimuli. Although no molecular information is available about this signal transduction pathway, it has been postulated that the altered conformation of PYP in pB causes an interaction with the corresponding site of a hypothetical receptor protein that mediates the negative phototactic response (Meyer et al., 1989; Sprenger et al., 1993). Therefore, this study establishes a link between the physical chemistry of protein folding and the (conformational) transitions in a photoreceptor protein.

We thank Erwin Peterman for technical support with the transient absorbance measurements and Rienk van Grondelle for his support and helpful comments on the manuscript.

Supported by the Dutch Organisation for Pure Research via the Foundation of Biological Research and by the Consortium für elektrochemische Industrie GmbH, Central Research Company of Wacker-Chemie GmbH, Munich, Germany.

REFERENCES

Baca, M., G. E. O. Borgstahl, M. Boissinot, P. M. Burke, W. R. Williams, K. A. Slater, and E. D. Getzoff. 1994. Complete chemical structure of the photoactive yellow protein: novel thioester-linked 4-hydroxycinnamyl chromophore and photocycle chemistry. *Biochemistry.* 33: 14369–14377.

Borgstahl, G. E. O., D. R. Williams, and E. D. Getzoff. 1995. 1.4 Å structure of photoactive yellow protein, a cytosolic photoreceptor: unusual fold, active site, and chromophore. *Biochemistry.* 34:6278–6287.

Brandts, J. F. 1964. The thermodynamics of protein denaturation. I. The denaturation of chymotrypsinogen. *J. Am. Chem. Soc.* 86:4291–4301.

Chen, B., W. A. Baase, and J. A. Schellman. 1989. Low-temperature unfolding of a mutant of phage T4 lysozyme. 2. Kinetic investigations. *Biochemistry.* 28:691–699.

Chen, B., and J. A. Schellman. 1989. Low-temperature unfolding of a mutant of phage T4 lysozyme. 1. Equilibrium studies. *Biochemistry.* 28:685–691.

Creighton, T. E. 1992. Folding pathways determined using disulfide bonds. *In* Protein Folding. T. E. Creighton, editor. Freeman, New York. 301–352.

Devault, D. 1980. Quantum mechanical tunneling in biological systems. *Q. Rev. Biophys.* 13:387–564.

Henderson, R., J. M. Baldwin, T. A. Ceska, F. Zemlin, E. Beckmann, and K. H. Downing. 1990. Model for the structure of bacteriorhodopsin based on high-resolution electron cryo-microscopy. *J. Mol. Biol.* 123: 899–929.

Henry, E. R., and J. Hofrichter. 1992. Singular value decomposition: application to analysis of experimental data. *Methods Enzymol.* 210: 129–192.

Hoff, W. D., P. Düx, K. Hård, B. Devreese, I. M. Nugteren-Roodzant, W. Crielaard, R. Boelens, R. Kaptein, J. J. Van Beeumen, and K. J. Hellingwerf. 1994a. Thiol ester-linked *p*-coumaric acid as a new photoactive prosthetic group in a protein with rhodopsin-like photochemistry. *Biochemistry.* 33:13959–13962.

Hoff, W. D., S. L. S. Kwa, R. Van Grondelle, and K. J. Hellingwerf. 1992. Low temperature absorption and fluorescence spectroscopy of the photoactive yellow protein from *Ectothiorhodospira halophila. Photochem. Photobiol.* 56:529–539.

Hoff, W. D., W. W. Sprenger, P. W. Postma, T. E. Meyer, M. Veenhuis, T. Leguijt, and K. J. Hellingwerf. 1994b. The photoactive yellow protein from *Ectothiorhodospira halophila* as studied with a highly specific polyclonal antiserum: (intra)cellular localization, regulation of expression, and taxonomic distribution of cross-reacting proteins. *J. Bacteriol.* 176:3920–3927.

Hoff, W. D., I. H. M. Van Stokkum, H. J. Van Ramesdonk, M. E. Van Brederode, A. M. Brouwer, J. C. Fitch, T. E. Meyer, R. Van Grondelle, and K. J. Hellingwerf. 1994c. Measurement and global analysis of the absorbance changes in the photocycle of the photoactive yellow protein from *Ectothiorhodospira halophila. Biophys. J.* 67:1691–1705.

Jackson, S. E., and A. R. Fehrst. 1991. Folding of chymotrypsin inhibitor 2. 2. Influence of proline isomerization on the folding kinetics and thermodynamic characterization of the transition state of folding. *Biochemistry.* 30:10436–10443.

Laidler, K. J. 1987. Chemical Kinetics. Harper and Row, New York.

Makhatadze, G. I., and P. L. Privalov. 1990. Heat capacity of proteins. I. Partial molar heat capacity of individual amino acid residues in aqueous solution: hydratation effect. *J. Mol. Biol.* 213:375–384.

Malinowski, E. R. 1991. Factor Analysis in Chemistry, 2nd Ed. Wiley, New York.

McRee, D. E., J. A. Tainer, T. E. Meyer, J. J. Van Beeumen, M. A. Cusanovich, and E. D. Getzoff. 1989. Crystallographic structure of a photoreceptor protein at 2.4 Å resolution. *Proc. Natl. Acad. Sci. USA.* 86:6533–6537.

Meyer, T. E. 1985. Isolation and characterization of soluble cytochromes, ferredoxins and other chromophoric proteins from the halophilic phototrophic bacterium *Ectothiorhodospira halophila. Biochim. Biophys. Acta.* 806:175–183.

Meyer, T. E., J. C. Fitch, R. G. Bartch, G. Tollin, and M. A. Cusanovich. 1990. Soluble cytochromes and a photoactive yellow protein isolated from the moderately halophilic purple phototrophic bacterium, *Rhodospirillum salexigens. Biochim. Biophys. Acta.* 1016:364–370.

Meyer, T. E., G. Tollin, T. P. Causgrove, P. Cheng, and R. E. Blankenschip. 1991. Picosecond decay kinetics and quantum yield of fluorescence of the photoactive yellow protein from the halophilic purple phototrophic bacterium, *Ectothiorhodospira halophila. Biophys. J.* 59: 988–991.

Meyer, T. E., G. Tollin, J. H. Hazzard, and M. A. Cusanovich. 1989. Photoactive yellow protein from the purple phototrophic bacterium, *Ectothiorhodospira halophila.* Quantum yield of photobleaching and effects of temperature, alcohols, glycerol, and sucrose on kinetics of photobleaching and recovery. *Biophys. J.* 56:559–564.

Meyer, T. E., E. Yakali, M. A. Cusanovich, and G. Tollin. 1987. Properties of a water-soluble, yellow protein isolated from a halophilic phototrophic bacterium that has photochemical activity analogous to sensory rhodopsin. *Biochemistry.* 26:418–423.

Mizutani, Y., S. Tokutomi, S. Kaminaka, and T. Kitagawa. 1993. Ultraviolet resonance Raman spectra of pea intact, large, and small phytochromes: differences in molecular topography of the red- and far-red-absorbing forms. *Biochemistry.* 32:6916–6922.

Ng, K., E. D. Getzoff, and K. Moffat. 1995. Optical studies of a bacterial photoreceptor protein, photoactive yellow protein, in single crystals. *Biochemistry.* 34:879–890.

Pace, C. N. 1990. Conformational stability of globular proteins. *Trends Biochem. Sci.* 15:14–17.

Privalov, P. L. 1979. Stability of proteins. Small globular proteins. *Adv. Protein Chem.* 33:167–241.

Privalov, P. L. 1988. Stability of protein structure and hydrophobic interaction. *Adv. Protein Chem.* 39:191–234.

Privalov, P. L. 1992. Physical basis of the stability of the folded conformations of proteins. *In* Protein Folding. T. E. Creighton, editor. W. H. Freeman and Company, New York. 83–126.

Privalov, P. L., and G. I. Makhatadze. 1990. Contribution of hydration and non-covalent interactions to the heat capacity effect on protein unfolding. *J. Mol. Biol.* 224:715–723.

Privalov, P. L., and S. A. Pothekin. 1986. Scanning microcalorimetry in studying temperature-induced changes in proteins. *Methods Enzymol.* 131:4–51.

Provencher, S. W. 1982. A constrained regularization method for inverting data represented by linear algebraic or integral equations. *Comput. Phys. Commun.* 27:213–227.

Provencher, S. W., and R. H. Vogel. 1980. Information loss with transform methods in system identification: a new set of transforms with high information content. *Math. Biosci.* 50:251–262.

Pullerits, T., F. Van Mourik, R. Monshouwer, R. W. Visschers, and R. Van Grondelle. 1994. Electron-phonon coupling in the B820 subunit of LH1 studied by temperature dependence of optical spectra. *J. Luminescence.* 58:168–171.

Rath, P., L. L. J. DeCaluwé, P. H. M. Bovee-Geurts, W. J. DeGrip, and K. J. Rothschild. 1993. Fourier transform infrared difference spectroscopy of rhodopsin mutants: light activation of rhodopsin causes hydrogen-bonding change in residue aspartic acid-83 during meta II formation. *Biochemistry.* 32:10275–10282.

Resek, J. F., Z. T. Farahbakhsh, W. L. Hubbel, and H. G. Khorana. 1993. Formation of the meta II photointermediate is accompanied by conformational changes in the cytoplasmatic surface of rhodopsin. *Biochemistry.* 32:12025–12032.

Ross, D. L., and J. Blanck. 1971. *In* Photochromism. G. H. Brown, editor. Wiley Interscience, New York. 471–556.

Salamon, Z., T. E. Meyer, and G. Tollin. 1995. Photobleaching of the photoactive yellow protein from *Ectothiorhodospira halophila* promotes binding to lipid bilayers: evidence from surface plasmon resonance spectroscopy. *Biophys. J.* 68:648–654.

Segawa, S., and M. Sugihara. 1984. Characterization of the transition state of lysozyme unfolding. I. Effect of protein-solvent interactions on the transition state. *Biopolymers.* 23:2473–2488.

Sprenger, W. W., W. D. Hoff, J. P. Armitage, and K. J. Hellingwerf. 1993. The eubacterium *Ectothiorhodospira halophila* is negatively phototactic with a wavelength dependence that fits the absorption spectrum of the photoactive yellow protein. *J. Bacteriol.* 175:3096–3104.

Spudich, J. L., and R. A. Bogomolni. 1988. Sensory rhodopsins of Halobacteria. *Annu. Rev. Biophys. Biophys. Chem.* 17:193–215.

Stavenga, D. G., J. Schwemer, and K. J. Hellingwerf. 1991. Visual pigments, bacterial rhodopsins and related retinoid-binding proteins. *In* Photoreceptor Evolution and Function. M. G. Holmes, editor. Academic Press, London. 261–349.

Subramaniam, S., M. Gerstein, D. Oesterhelt, and H. Henderson. 1993. Electron diffraction analysis of structural changes in the photocycle of bacteriorhodopsin. *EMBO J.* 12:1–8.

Toossi, Z., Z. T. Farahbakhsh, K. Hideg, and W. L. Hubbell. 1993. Photoactivated conformational changes in rhodopsin: a time-resolved spin-label study. *Science.* 262:1416–1419.

Van Beeumen, J. J., B. Devreese, S. Van Bun, W. D. Hoff, K. J. Hellingwerf, T. E. Meyer, D. E. McRee, and M. A. Cusanovich. 1993. The primary structure of a photoactive yellow protein from the phototrophic bacterium, *Ectothiorhodospira halophila*, with evidence for the mass and the binding site of the chromophore. *Protein Sci.* 2:1114–1125.

Van Brederode, M. E., Th. Gensch, W. D. Hoff, K. J. Hellingwerf, and S. E. Braslavsky. 1995. Photoinduced volume changes and energy storage associated with the early transformations of the photoactive yellow protein from *Ectothiorhodospira halophila. Biophys. J.* 68:1101–1109.

Van Stokkum, I. H. M., A. M. Brouwer, H. J. Van Ramesdonk, and T. Scherer. 1993. Multiresponse parameter estimation and compartmental analysis of time resolved fluorescence spectra. Application to conformational dynamics of charge-separated species in solution. *Proc. K. Ned. Akad. Wet.* 96:43–68.

Van Stokkum, I. H. M., T. Scherer, A. M. Brouwer, and J. W. Verhoeven. 1994. Conformational dynamics of flexibly and semirigidly bridged electron donor-acceptor systems as revealed by spectrotemporal parameterization of fluorescence. *J. Phys. Chem.* 98:852–866.

Váró, G., and K. J. Lanyi. 1991. Thermodynamics and energy coupling in the bacteriorhodopsin photocycle. *Biochemistry.* 30:5016–5022.

Weese, J. 1992. A reliable and fast method for the solution of Fredholm integral equations of the first kind based on Tikhonov regularization. *Comput. Phys. Commun.* 69:99–111.

Wells, T. A., M. A. Nakazawa, K. Manabe, and P. S. Song. 1994. A conformational change associated with the phototransformation of *Pisum* phytochrome A as probed by fluorescence quenching. *Biochemistry.* 33:708–712.

Xie, D., V. Bhakuni, and E. Freire. 1991. Calorimetric determination of the energetics of the molten globule intermediate in protein folding: apo-α-lactalbumin. *Biochemistry.* 30:10673–10678.

Yamamoto, K. T. 1993. Photoreversible change in the conformation of phytochrome as probed with a covalently bound fluorescent sulfhydryl reagent, *N*-(9-acridinyl)maleimide. *Biochim. Biophys. Acta.* 1163: 227–233.

Yan, B., K. Nakanishi, and J. L. Spudich. 1991a. Mechanism of activation of sensory rhodopsin I: evidence for a steric trigger. *Proc. Natl. Acad. Sci. USA.* 88:9412–9416.

Yan, B., T. Takahasi, R. Johnson, and J. L. Spudich. 1991b. Evidence that the repellent receptor form of sensory rhodopsin I is an attractant signaling state. *Biochemistry.* 30:10686–10692.